A State Feedback Controller for PMSMs Based on Penalty Term Augmented Seeker Optimization Algorithm

Changchang Hu
Automotive Engineering Research Institute
Jiangsu University
Zhenjiang, China
huchangchang_jd@163.com

Xiaodong Sun*
Automotive Engineering Research Institute
Jiangsu University
Zhenjiang, China
xdsun@ujs.edu.cn

Zebin Yang
Automotive Engineering Research Institute
Jiangsu University
Zhenjiang, China
zbyang@ujs.edu.cn

Gang Lei
School of Electrical and Data Engineering
University of Technology Sydney
Sydney, Australia
gang.lei@uts.edu.au

Youguang Guo
Automotive Engineering Research Institute
Jiangsu University
Zhenjiang, China
youguang.guo-1@uts.edu.au

Jianguo Zhu
School of Electrical and Information Engineering
The University of Sydney
Sydney, Australia
jianguo.zhu@sydney.edu.au

***Abstract*—This paper presents the design of a state feedback controller (SFC) for permanent-magnet synchronous motor (PMSM) drive. First, in order to ensure null steady-state error in speed and zero d-axis current, the discretized state space model of PMSM is augmented with integral of rotor speed error and *d*-axis current error. Then, the seeker optimization algorithm (SOA) is employed to get the parameters of the proposed SFC. Furthermore, a penalty term is introduced to the fitness index to suppress overshoots. Finally, the SOA based SFC with and without penalty term are compared in experiments.**

Keywords—Permanent magnet (PM) synchronous motor, PM hub motor, state feedback controller, seeker optimization algorithm

I. INTRODUCTION

With the worldwide environment deterioration, the improvement of energy efficiency has become increasingly important. Compared to traditional internal combustion engine vehicles, electrical vehicles (EVs) have higher energy efficiency and lower emissions. With the advantages of short drive chain, high dynamic performance and high efficiency, the permanent-magnet synchronous hub motors (PMSHMs) are considered alternative to the traditional permanent-magnet synchronous motor (PMSM) system with mechanical transmission for EVs [1]-[6].

The vector control system often adopts cascade control structure including two PI loops. The PI controllers has advantages of simple algorithm, good robustness and high reliability. However, for cascade controller structures, the existence of inner control loop will deteriorate the dynamical properties of the drive [7].

While the SFC control system can handle all the variables of PMSM drive with one controller, overcoming the drawback of the cascaded control structure naturally [8]-[12]. Augmented with intelligent algorithm, the performance of SFC can be improved significantly [13], [14].

SOA is a relatively novel swarm intelligence optimization method, due to the advantage of simple principle, good convergence capability and high solution accuracy [15], [16], it is thought to be suitable for solving optimal problems.

II. LINEARIZATION OF PMSHM MODEL

In order to apply SFC to the control of PMSM drive, the motor model needs to be linearized first.

The nonlinear mathematical model of the surface mounted PMSHM in *dq*-axis reference rotor frame can be expressed as:

$$\begin{cases} u_{sd} = R_s i_d + L_s \dfrac{d}{dt} i_{sd} - p\omega_m L_s i_{sq} \\ u_{sq} = R_s i_q + L_s \dfrac{d}{dt} i_{sq} + p\omega_m (L_s i_{sd} + \psi) \end{cases} \tag{1}$$

$$\frac{d}{dt}\omega_m = \frac{1}{J}\left(\frac{3}{2} p\psi i_{sq} - B_m\omega_m - T_l\right) \tag{2}$$

where Rs, Ls, and ψ are the resistance, inductance, and the magnetic flux of the PMSHM, respectively, u_{sq} and u_{sd} are the *q*-axis and d-axis voltages, respectively, ω_m is rotor speed, *p* is the pole pair numbers, and B_m is viscous friction.

In order to obtain a linearized PMSHM model, two variables are defined as

$$u_{md}(t) = -p\omega_m L_s i_q \tag{3}$$

$$u_{mq}(t) = p\omega_m (L_s i_d + \psi) \tag{4}$$

By substituting (3) and (4) into (1), the following expression can be obtained.

$$\begin{cases} u_{ld} = R_s i_d + L_s \dfrac{d}{dt} i_{sd} \\ u_{lq} = R_s i_q + L_s \dfrac{d}{dt} i_{sq} \end{cases} \tag{5}$$

where $\begin{bmatrix} u_{ld} \\ u_{lq} \end{bmatrix} = \begin{bmatrix} u_{sd} \\ u_{sq} \end{bmatrix} - \begin{bmatrix} u_{md} \\ u_{mq} \end{bmatrix}$. Then the model of PMSHM given by (2) and (5) can be described in a standard form of a linear state equation as follows:

$$\frac{d}{dt}\boldsymbol{x}(t)=\boldsymbol{A}\boldsymbol{x}(t)+\boldsymbol{B}\boldsymbol{u}_l(t)+\boldsymbol{E}d(t) \tag{6}$$

where

$$\boldsymbol{A}=\begin{bmatrix}-\frac{R_s}{L_s} & 0 & 0\\ 0 & -\frac{R_s}{L_s} & 0\\ 0 & \frac{3p\psi}{2J_m} & -\frac{B_m}{J_m}\end{bmatrix},\ \boldsymbol{B}=\begin{bmatrix}\frac{1}{L_s} & 0\\ 0 & \frac{1}{L_s}\\ 0 & 0\end{bmatrix},\ \boldsymbol{E}=\begin{bmatrix}0\\ 0\\ -\frac{1}{J_m}\end{bmatrix},$$

$$\boldsymbol{x}(t)=\begin{bmatrix}i_{sd}(t)\\ i_{sq}(t)\\ \omega_m(t)\end{bmatrix},\ \boldsymbol{u}_l(t)=\begin{bmatrix}u_{ld}\\ u_{lq}\end{bmatrix},\ d(t)=T_l(t)$$

III. SPEED CONTROLLER DESIGN

For linearized systems, the state feedback control law can be expressed as

$$\boldsymbol{u}(t)=-\boldsymbol{K}\boldsymbol{x}(t) \tag{7}$$

where $\boldsymbol{u}(t)$ represents control variables, $\boldsymbol{x}(t)$ is system state, $\boldsymbol{K}$ is the feedback gain.

In order to improve steady state performance of the proposed SFC, integral terms are needed to be added into the system model. Different from conventional single-motor drive systems, hub motors are usually adopted in distributed drive vehicles, which means the speed error is directly related to the vehicle safety and need to be strictly limited. Also, MTPA strategy is employed in this drive. Thus, the integral of speed error and integral of i_d error are added into the system model.

$$e_{id}=\int(i_d-i_d^{\,ref})dt \tag{8}$$

$$e_{\omega}=\int(\omega_m-\omega^{ref})dt \tag{9}$$

The augmented state variable matrix is

$$\bar{\boldsymbol{x}}(t)=\begin{bmatrix}i_{sd}(t) & i_{sq}(t) & \omega_m(t) & e_{id}(t) & e_{\omega}(t)\end{bmatrix}^{\mathrm{T}} \tag{10}$$

where ω_m and i_d are rotor speed and d-axis current. ω^{ref} and i_d^{ref} are their reference values.

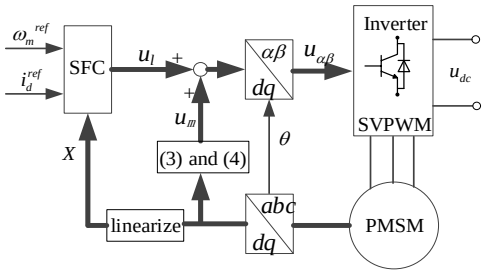

Fig.1. Block diagram of PMSHM drive with proposed SFC

In order to implement this speed controller in dSPACE platform, a discrete form of control law is designed.

$$\boldsymbol{u}(n)=-\boldsymbol{K}_d\bar{\boldsymbol{x}}(n)=-\boldsymbol{K}_{dx}\boldsymbol{x}(n)-\boldsymbol{K}_{de}\boldsymbol{x}_e(n) \tag{11}$$

where $\boldsymbol{K}_d$ is the gain matrix of the SFC

$$\boldsymbol{K}_d=[\boldsymbol{K}_{dx}\ \boldsymbol{K}_{de}]=\begin{bmatrix}K_{dx1} & K_{dx2} & K_{dx3} & K_{de1} & K_{de2}\\ K_{dx4} & K_{dx5} & K_{dx6} & K_{de3} & K_{de4}\end{bmatrix}$$

The block diagram of proposed drive with SFC is shown in Fig. 1.

In order to select gain matrix automatically with the SOA, the fitness index should firstly be designed. As the control objectives are 1) zero d-axis current and 2) zero speed error, the following fitness index has been designed:

$$F_1=\frac{1}{N}\sum_{n=0}^{N}[|\Delta e_{\omega}(n)|nTs+|\Delta e_{id}(n)|nTs)] \tag{12}$$

where Ts is the sampling period, and n is discrete sample time index. In order to suppress overshoot more efficiently, the penalty term λ is added to the function:

$$F_2=\frac{1}{N}\sum_{n=0}^{N}[|\Delta e_{\omega}(n)|nTs+|\Delta e_{id}(n)|nTs+\lambda\Delta e_{\omega}(n)nTs] \tag{13}$$

with $\Delta e_{\omega}(n)=\omega_m(n)-\omega^{ref}(n)$, $\Delta e_{id}(n)=i_d(n)-i_d^{\,ref}(n)$.

The overshoot error cumulative value after 40 iterations is defined as a comparison criterion to select an appropriate value for the penalty term λ.

$$OECV=\sum_{n_1}^{n_2}e_{\omega}(n) \tag{14}$$

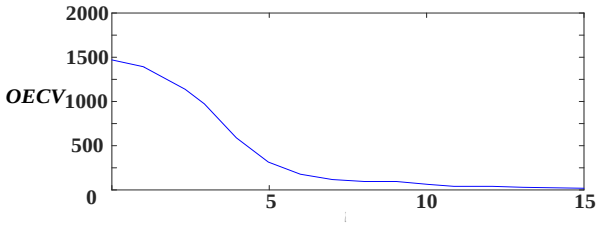

Fig. 2. *OECV* with different λ

The value of *OECV* with λ from 0 to 15 are shown in Fig.2, as can be observed that, when λ is greater than 11, the speed overshoot can be effectively suppressed. Therefore, λ=14 is taken in this paper.

IV. SOA

The SOA algorithm is based on the study of human random intelligent search behavior. Apply this intelligent behavior to the search for problem-optimized solutions. Combined with the idea of human evolution, the uncertain reasoning of the human search is used to determine the search step length and the empirical gradient is used to determine the search step direction, and then the seeker position update is completed to optimize the problem.

A. Determination of search direction

The direction update of SOA algorithm depends on egotistical direction, altruistic direction and proactive direction. The update strategy is shown in

$$\vec{d}_i(t)=sign(\omega\vec{d}_{i,pro}+\varphi_1\vec{d}_{i,ego}+\varphi_2\vec{d}_{i,alt}) \tag{15}$$

where ω is the inertia weight, it will linearly decrease from 0.9 to 0.1 as the evolution grows. φ_1, φ_2 are random weights between 0 and 1. $d_{i,pro}$ is the proactive direction, $d_{i,ego}$ is the egotistical direction, and $d_i$alt is the altruistic direction. They are:

$$\begin{cases} \overrightarrow{d}_{i,ego}(t) = \overrightarrow{p}_{i,best} - \overrightarrow{x}_i(t) \\ \overrightarrow{d}_{i,alt}(t) = \overrightarrow{g}_{i,best} - \overrightarrow{x}_i(t) \\ \overrightarrow{d}_{i,pro}(t) = \overrightarrow{x}_i(t_1) - \overrightarrow{x}_i(t_2) \end{cases} \quad (16)$$

where sign(g) is signum function, $p_{i,best}$ is the best position for the seeker with index i, $g_{i,best}$ is the best position among its fellow neighbor seekers, and $\vec{x}_i(t_1), \vec{x}_i(t_2)$ are the best two positions in $\{\vec{x}_i(t\text{-}1), \quad \vec{x}_i(t\text{-}2), \quad \vec{x}_i(t)\}$.

B. Determination of search step length

The uncertain reasoning behavior of SOA is to use the approximation ability of fuzzy system to simulate the intelligent searching behavior of human to establish the relationship between perception (i.e., the value of objective function) and behavior (i.e., step size). Gaussian membership function is adopted to represent the fuzzy variable of search step size:

$$u_A(x) = e^{-(x-u)^2/2\delta^2} \quad (17)$$

where u_A is Gaussian membership, x is the input variable; δ, u is the membership function parameter. u_{min} is set to 0.0111. Linear membership function is adopted to make the membership directly proportional to the order of function values, i.e., the maximum membership value u_{max} = 1 in the best position. The worst position has minimum membership u_{min} = 0. 0111, at another places u is less than 1.0, as shown in follow:

$$u_{ij} = rand(u_i, 1),\ j = 1, 2, \cdots D \quad (18)$$

where u_i is the membership of the target function value i, u_{ij} is the membership of the target function value i in the j-dimensional search space, D is the dimension of search space.

V. AUTO TUNING OF SFC

In auto tuning procedure, the fitness value is expected to be decreased with iterations grows. The trend of fitness value will directly reflect the convergence of SOA. Also, as is defined in (12) and (13), smaller fitness value can only be obtained by smaller speed error and i_d error. Which means a better controller performance.

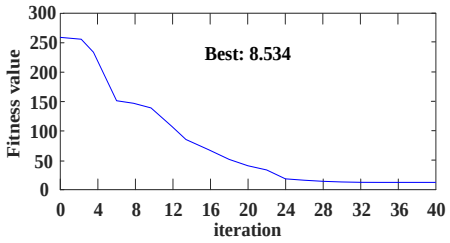

Fig3 Evolution of F_1 during auto-tuning procedure

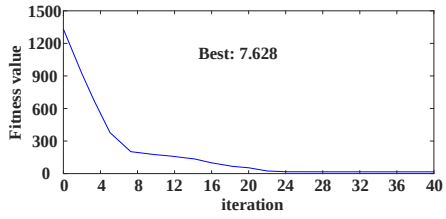

Fig4 Evolution of F_2 during auto-tuning procedure

The autotuning task is implemented in MATLAB R2016a environment, on a PC with i5-4200 CPU @ 2.5 GHz with 8GB RAM. The overall trend of F_1 during parameter tuning process with SOA are shown in Figs.3. The evolution of F_2 with SOA is recorded in Fig.4.

It should be noted that, due to the introduction of penalty term, the initial value of F_2 is very large (as in Fig.4), but it decreases rapidly in following iterations. When iterated 20 times, the difference between F_2 and F_1 has become very small, and after 40 iterations, they are approximately the same. The best fitness indexes after 40 iterations are F_1=8.534 and F_2=7.628, respectively. Figs. 5 and 6 show the evolution of speed during the auto tuning procedure with F_1 and F_2 (ω_{ref} = 350 rpm, Tl = 10 Nm at t = 0.2 s).

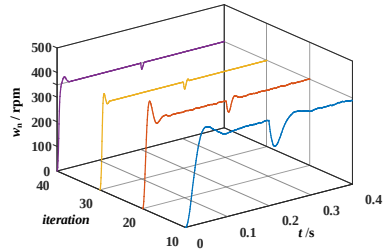

Fig.5. Evolution of speed during auto-tuning procedure with F_1

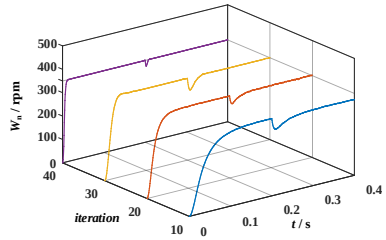

Fig.6. Evolution of speed during auto-tuning procedure with F_2

The final values of gain matrices obtained after 40 iterations are as follows

$$K_1 = \begin{bmatrix} 263.2 & 0 & 0 & 0 & 73.17 \\ 0 & 0.5 & 0.0358 & 0.651 & 0 \end{bmatrix},$$

$$K_2 = \begin{bmatrix} 160.53 & 0 & 0 & 0 & 60.65 \\ 0 & 1.75 & 0.0432 & 0.44 & 0 \end{bmatrix}$$

It is worth to point out that the element value of K_1[2,2] and K_2[2,2] represent the sensitive of the controllers to variant i_q. Greater value means controller will give more attention on this variant. Thus, if the same control voltage is required in some transient instant for SFC with $\boldsymbol{K_1}$ (SFC1) and SFC with $\boldsymbol{K_2}$ (SFC2), i_q in SFC2 may be smaller than that in SFC1. This assumption will be verified in the following experiments.

VI. EXPERIMENTAL RESULTS

To validate the system performance with the proposed controller, experiments are carried out on the dSPACE ds1401 platform, experimental setup is shown in Fig.7.

In order to compare the proposed SFCs, two test cases are studied. In case 1, the reference speed is set to 350 rpm, the load torque is initially set to zero, and turns to 10 Nm at 0.2s. The speed and current responses of SFC1 and SFC2 are recorded in Fig.8(a) and Fig.8(b). In test case 2, the reference speed is set to be the same as in test case 1, but the load condition in this case is contrary to case1, i.e., the load torque is initially set to 10 Nm, and removed at 0.2s. The speed and current response in this case are shown in Fig 9 (a) and (b). The maximum of i_q is set to 10A in both cases to ensure safety.

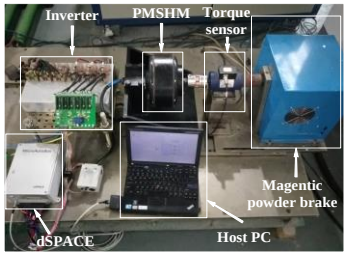

Fig7 Experimental setup

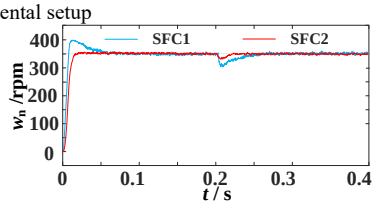

(a)

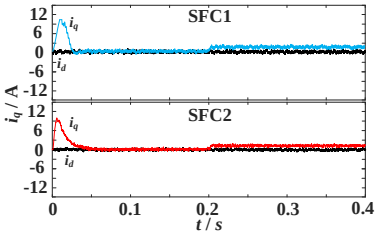

(b)

Fig. 8. Experimental results (a) Speed (b) Currents

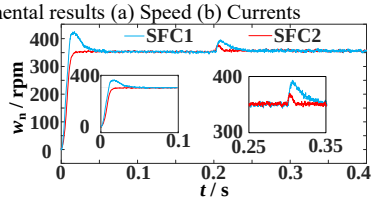

(a)

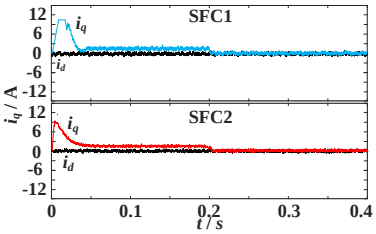

(b)

Fig. 8. Experimental results (a) Speed (b) Currents

As shown in upon figures, both SFC1 and SFC2 can track reference speed without steady-state error in two load conditions. SFC1 has a slightly faster response speed than SFC2. However, as it is obviously shown in these figures, there is a relatively large overshoot in SFC1 speed response, but for SFC2, thanks to the introduction of penalty term λ in F_2, it allows tracking reference speed almost without any overshoot. Moreover, as can be observed from current curves, both in Fig. 8(b) and in Fig. 9 (b), the i_q in SFC1 has reached the peak value, this will cause the windup problem and deteriorate the controller dynamic property.

VII. CONCLUSION

This paper presented a SOA based SFC for high performance control of PMSM. By introducing two integrals to state variable matrix, the steady-state error in speed tracking is eliminated and *d*-axis current is fixed to zero. Also, a penalty term is added to the traditional fitness index to suppress overshoots and improve dynamic property. And the experimental results indicate that the performance of the proposed SFC2 is better than SFC1.

ACKNOWLEDGMENT

This work was supported by the National Natural Science Foundation of China under Project 51875261, the Natural Science Foundation of Jiangsu Province of China under Projects BK20180046 and BK20170071, the "Qinglan project" of Jiangsu Province, the Key Project of Natural Science Foundation of Jiangsu Higher Education Institutions under Project 17KJA460005, the Six Categories Talent Peak of Jiangsu Province under Project 2015-XNYQC-003, and the Postgraduate Research & Practice Innovation Program of Jiangsu Province under Project SJCX18_0745.

REFERENCES

[1] T. Wu et al., "Multiobjective optimization of a tubular coreless LPMSM based on adaptive multiobjective black hole algorithm," *IEEE Trans. Ind. Electron.* doi: 10.1109/TIE.2019.2916347

[2] G. Lei, W. Xu, J. Hu, J. Zhu, Y. Guo and K. Shao, "Multilevel design optimization of a FSPMM drive system by using sequential subspace optimization method," *IEEE Trans. Magn.*, vol. 50, no. 2, pp. 685-688, Feb. 2014.

[3] X. Sun, K. Diao, G. Lei, L. Chen, Y. Guo and J. Zhu, "Study on segmented-rotor switched reluctance motors with different rotor pole numbers for BSG system of hybrid electric vehicles," *IEEE Trans. Veh. Technol.*, doi: 10.1109/TVT.2019.2913279

[4] A. Dalal and P. Kumar, "Design, prototyping, and testing of a dual-rotor motor for electric vehicle application," *IEEE Trans. Ind. Electron*, vol. 65, no. 9, pp. 7185-7192, Sept. 2018.

[5] Z. Ke, J. Zhang, and M. W. Degner, "DC bus capacitor discharge of permanent-magnet synchronous machine drive systems for hybrid electric vehicles," *IEEE Trans. Ind. Appl.*, vol.53, no.2, pp.1399–1405, Mar./Apr. 2017.

[6] P. Zheng, Y. Sui, J. Zhao, C. Tong, T. Lipo, and A. Wang, "Investigation of a novel five-phase modular permanent-magnet in-wheel motor," *IEEE Trans. Magn.*, vol. 47, no. 10, pp. 4084-4087, Oct. 2011.

[7] M. Preindl and S. Bolognani, "Model predictive direct speed control with finite control set of PMSM drive systems," *IEEE Trans. Power Electron.*, vol. 28, no. 2, pp. 1007-1015, Feb. 2013

[8] S. Agarwal, D. Yadav, and A. Verma, "Speed control of PMSM drive using bacterial foraging optimization," in *Proc. IEEE Uttar Pradesh Section Int. Conf. Electrical, Computer and Electronics (UPCON)*, 2017, pp. 84-90.

[9] C. J. Meirinho, A. Bartsch, J. de Oliveira and M. S. M. Cavalca, "An optimal MIMO control approach for PMSM drives," in Proc. Brazilian Power Electron. Conf. (COBEP), 2017, pp. 1-6.

[10] M. Brasel, "A gain-scheduled multivariable LQR controller for permanent magnet synchronous motor," in *Proc. 19th Int. Conf. Methods Models Auto. Robot. (MMAR)*, 2014, pp. 722-725.

[11] P. Teppa Garran, V. Nardone, and J. Rodriguez Diez, "LQR control employing output derivative measures," *IEEE Latin America Trans.*, vol. 13, no. 8, pp. 2538-2544, Aug. 2015.

[12] T. K. Boukas and T. G. Habetler, "High-performance induction motor speed control using exact feedback linearization with state and state derivative feedback," *IEEE Trans. Power Electron.*, vol. 19, no. 4, pp. 1022-1028, July 2004.

[13] B. Ufnalski, A. Kaszewski, and L. M. Grzesiak, "Particle swarm optimization of the multioscillatory LQR for a three-phase four-wire voltage-source inverter with an LC output filter," *IEEE Trans. Ind. Electron.*, vol. 62, no. 1, pp. 484-493, Jan. 2015

[14] K. Paponpen and M. Konghirun, "LQR state feedback controller based on particle swarm optimization for IPMSM drive system," in *Proc. IEEE 10th Conf. Ind. Electron. Appl. (ICIEA)*, 2015, pp. 1175-1180.

[15] C. Dai, W. Chen, Y. Song and Y. Zhu, "Seeker optimization algorithm: A novel stochastic search algorithm for global numerical optimization," *Journal of Systems Engineering and Electronics*, vol. 21, no. 2, pp. 300-311, Apr. 2010.

[16] J. Wan *et al.*, "Fractional order PID motion control based on seeker optimization algorithm for AUV," *OCEANS 2018 MTS/IEEE Charleston*, 2018, pp. 1-4.